AD-A037 932 COLD REGIONS RESEARCH AND ENGINEERING LAB HANOVER N H F/G 8/13
EFFECT OF TEMPERATURE ON THE STRENGTH OF FROZEN SILT,(U)
FEB 77 F D HAYNES, J A KARALIUS

UNCLASSIFIED CRREL-77-3 NL

1 OF 1
AD A037932

END

DATE FILMED
5-77

CRREL REPORT 77-3

Effect of temperature on the strength of frozen silt

For conversion of metric units to U.S./British customary units of measurement consult ASTM Standard E380, Metric Practice Guide, *published by the American Society for Testing and Materials, 1916 Race St., Philadelphia, Pa. 19103.*

Cover: Compression test, temperature 0°C, machine speed 4.23 cm/sec. (Photo by J. Karalius.)

CRREL Report 77-3

(12)

Effect of temperature on the strength of frozen silt

F. Donald Haynes and Jack A. Karalius

February 1977

Prepared for
DIRECTORATE OF MILITARY CONSTRUCTION
OFFICE, CHIEF OF ENGINEERS
By
CORPS OF ENGINEERS, U.S. ARMY
COLD REGIONS RESEARCH AND ENGINEERING LABORATORY
HANOVER, NEW HAMPSHIRE

Unclassified

SECURITY CLASSIFICATION OF THIS PAGE *(When Data Entered)*

REPORT DOCUMENTATION PAGE

READ INSTRUCTIONS BEFORE COMPLETING FORM

1. REPORT NUMBER: CRREL Report 77-3	2. GOVT ACCESSION NO.
3. RECIPIENT'S CATALOG NUMBER	
4. TITLE *(and Subtitle)*: EFFECT OF TEMPERATURE ON THE STRENGTH OF FROZEN SILT	5. TYPE OF REPORT & PERIOD COVERED
6. PERFORMING ORG. REPORT NUMBER	
7. AUTHOR(s): F. Donald Haynes and Jack A. Karalius	8. CONTRACT OR GRANT NUMBER(s)
9. PERFORMING ORGANIZATION NAME AND ADDRESS: U.S. Army Cold Regions Research and Engineering Laboratory, Hanover, New Hampshire 03755	10. PROGRAM ELEMENT, PROJECT, TASK AREA & WORK UNIT NUMBERS: DA Project 4A762719AT42, Task A2, Work Unit 004
11. CONTROLLING OFFICE NAME AND ADDRESS: Directorate of Military Construction, Office, Chief of Engineers, Washington, D.C. 20314	12. REPORT DATE: February 1977
	13. NUMBER OF PAGES: 33
14. MONITORING AGENCY NAME & ADDRESS *(if different from Controlling Office)*	15. SECURITY CLASS. *(of this report)*: Unclassified
	15a. DECLASSIFICATION/DOWNGRADING SCHEDULE

16. DISTRIBUTION STATEMENT *(of this Report)*

Approved for public release; distribution unlimited.

17. DISTRIBUTION STATEMENT *(of the abstract entered in Block 20, if different from Report)*

037 100

18. SUPPLEMENTARY NOTES

19. KEY WORDS *(Continue on reverse side if necessary and identify by block number)*

Compressive strength	Temperature effect
Fairbanks silt	Tensile strength
Frozen soil	Unfrozen water
Permafrost	Uniaxial tests
Strain rate	

20. ABSTRACT *(Continue on reverse side if necessary and identify by block number)*

Tests were conducted in uniaxial compression and tension to determine the effect of temperature on the strength of frozen Fairbanks silt. Test temperatures ranged from 0°C to -56.7°C. Two machine speeds, 4.23 cm/sec and 0.0423 cm/sec, were used for the constant displacement rate tests. From the highest to the lowest temperature, the compressive strength increased up to about one order of magnitude and the tensile strength increased one-half an order of magnitude. Equations are presented which correlate strength with temperature at the strain rates obtained. The initial tangent and 50% strength moduli and the specific energy are given for each test. The mode of fracture and the effects of unfrozen water content and ice matrix strengthening are discussed, and the test results are compared with the data of other investigations.

DD FORM 1 JAN 73 1473 EDITION OF 1 NOV 65 IS OBSOLETE

Unclassified

SECURITY CLASSIFICATION OF THIS PAGE *(When Data Entered)*

PREFACE

This report was prepared by F. Donald Haynes, Materials Research Engineer, Applied Research Branch, Experimental Engineering Division, U.S. Army Cold Regions Research and Engineering Laboratory (USA CRREL), and Jack A. Karalius, Civil Engineer, New Jersey State Highway Department, formerly Civil Engineering Assistant, USA CRREL.

The study covered by this report was performed under DA Project 4A762719AT42, *Design Construction and Operations Technology in Cold Regions*; Task A2, *Soils and Foundations Technology in Cold Regions*; Work Unit 004, *Excavation in Frozen Ground.*

Technical review of the report was performed by Dr. Malcolm Mellor, George W. Aitken, Francis H. Sayles, and Kevin L. Carey, all of USA CRREL.

The authors gratefully acknowledge the significant contributions made by many USA CRREL personnel. They extend special appreciation to Dr. Malcolm Mellor for assisting throughout the project and for reviewing this report. The authors are also grateful to George W. Aitken, Francis H. Sayles and Kevin L. Carey for reviewing the report, and to John Kalafut for providing valuable assistance with the instrumentation.

CONTENTS

ILLUSTRATIONS

TABLES

EFFECT OF TEMPERATURE ON THE STRENGTH OF FROZEN SILT

F. Donald Haynes and Jack A. Karalius

INTRODUCTION

Among the previous work done to determine the strength of frozen soil with uniaxial compression and tension tests was the investigation conducted by Haynes et al. (1975) concerning the effect of strain rate on the strength of a frozen silt. This was accomplished by holding the test temperature constant while varying the test machine speed. To supplement these results, another investigation was undertaken to establish the effect of temperature on the strength of the same silt; the findings are summarized in this report.

The purpose of this investigation was to determine the effect of temperature on the strength of frozen silt. This information is necessary for the development of excavation techniques to be used in frozen soil. In the investigation conducted by Haynes et al. (1975), the testing temperature was held constant at -9.4°C, while the machine speed was varied from 0.0021 cm/sec to 42.33 cm/sec. In the present investigation, a relatively fast machine speed of 4.23 cm/sec and a slow speed of 0.0423 cm/sec were used, while the testing temperature was varied from 0°C to -56.7°C. Tests were run on a relatively stiff, closed-loop, servo-controlled testing machine. A load cell was used for load measurements and linear variable differential transformer transducers were employed for deformation measurements on the dumbbell-shaped specimens.

In addition to the uniaxial compressive and tensile test results, the modulus, specific energy and activation energy were found and are discussed in this report. The uniaxial strength as a function of ice matrix strengthening and unfrozen water content is also discussed.

SAMPLE PREPARATION

The frozen soil samples were prepared in the same manner as described in the authors' previous report (see Haynes et al. 1975). The silt was obtained from the same source and was subjected to identical preparation processes. Its specific gravity was 2.71 and it can be classified in the ML group, a fine-grained, low-plasticity silt.

The preparation of frozen soil samples for testing was a careful, detailed process accomplished in the following steps:

1. assembling the mold
2. compacting the soil samples
3. saturating the samples
4. unidirectionally freezing the samples
5. disassembling the mold and removing the samples
6. preparing the samples for testing.

The 12.7- × 27.4- × 7.4-cm Lucite mold could form four 2.54-cm-diam × 8.26-cm-long samples at a time. Plastic inserts were placed in the cylinders of the mold to produce dumbbell-shaped samples. Aluminum end caps were placed in the mold and frozen onto the specimens during the freezing stage.

The soil was compacted in five layers using a 9.1-kg spring-loaded hammer and dealing 25 blows/layer. The ramming rod of the hammer had a 1.27-cm diameter and an area of 1.29 cm^2. Each layer was scarified to a depth of approximately 0.64 cm before the addition of the next layer. The soil was compacted in its air-dried state, about 1.5% moisture content by weight. This technique and compactive effort proved to be effective and yielded the desired properties of the samples, e.g., 1.43 g/cm^3 dry density, 0.90 void ratio, and 29% moisture content after saturation and freezing. Tables I and II contain the density, water content, degree of saturation, and void ratio of the compression and tension test samples respectively.

After completion of the compaction process, adapters were screwed into the threaded aluminum end caps at each end of the sample. Filter paper and porous stone were wedged into the adapters to prevent

Table I. Fairbanks silt specimen data for compression tests.

Test	Dry density (g/cm^3)	Wet density (g/cm^3)	Water content (%)	Degree of saturation (%)	Void ratio
1	1.42	1.84	29.9	96.1	0.914
2	1.41	1.83	29.3	93.8	0.916
3	1.38	1.81	31.0	94.9	0.960
4	1.44	1.85	28.1	94.0	0.876
5	1.42	1.85	29.9	97.1	0.904
6	1.44	1.85	29.1	96.6	0.884
7	1.39	1.82	31.0	95.5	0.953
8	M*	M	31.4	M	M
9	1.44	1.87	29.7	98.9	0.882
10	1.44	1.86	29.2	96.7	0.888
11	1.47	1.90	29.3	100.0	0.851
12	1.48	1.90	28.5	94.3	0.911
13	1.39	1.82	31.6	96.9	0.959
14	1.43	1.86	30.1	98.4	0.901
15	1.42	1.85	29.7	96.9	0.903
16	1.41	1.83	29.6	94.8	0.918
17	1.43	1.84	28.7	95.0	0.890
18	M	M	31.1	M	M
19	M	M	29.8	M	M
20	M	M	28.5	M	M
21	M	M	31.5	M	M
22	1.45	1.85	27.5	92.9	0.872
23	1.47	1.88	28.0	97.2	0.848
24	1.43	1.85	29.1	95.8	0.894
25	1.42	1.84	29.3	94.8	0.909
26	1.45	1.85	27.9	94.6	0.868
27	1.42	1.84	29.9	97.2	0.906
28	1.43	1.84	29.1	95.7	0.895
29	1.44	1.85	28.7	94.6	0.901
30	1.46	1.87	28.3	95.3	0.877
31	1.41	1.84	30.3	95.4	0.939
32	1.43	1.85	29.9	96.0	0.919
33	1.40	1.82	30.0	92.8	0.957
34	1.42	1.83	28.2	90.3	0.922
35	1.42	1.83	28.4	90.3	0.928
36	1.41	1.81	28.0	86.5	0.938
37	1.41	1.82	29.3	90.1	0.943
38	1.42	1.82	28.3	87.8	0.933
39	1.37	1.78	29.8	86.7	0.996
40	1.41	1.83	29.8	91.3	0.945
41	1.41	1.82	29.6	90.6	0.947
42	1.41	1.83	29.5	91.4	0.935
43	1.40	1.81	29.3	88.9	0.955
44	M	M	28.8	M	M
45	M	M	M	M	M
46	1.45	1.87	28.8	97.5	0.867
47	1.45	1.86	28.2	94.6	0.874

** M — data missing.*

Table I (cont'd).

Test	Dry density (g/cm^3)	Wet density (g/cm^3)	Water content (%)	Degree of saturation (%)	Void ratio
48	1.42	1.85	30.1	97.6	0.905
49	1.37	1.80	30.9	92.5	0.995
50	1.46	1.88	28.6	97.2	0.876
51	1.50	1.90	26.6	95.9	0.825
52	1.43	1.86	30.0	97.9	0.912
53	1.45	1.87	28.7	95.7	0.890
54	1.47	1.88	27.6	94.7	0.865

Table II. Fairbanks silt specimen data for tension tests.

Test	Dry density (g/cm^3)	Wet density (g/cm^3)	Water content (%)	Degree of saturation (%)	Void ratio
1	1.43	1.85	28.8	94.8	0.892
2	1.44	1.85	29.1	96.3	0.886
3	1.44	1.85	28.7	95.4	0.883
4	1.43	1.84	29.0	95.4	0.892
5	1.45	1.86	28.3	95.5	0.871
6	1.44	1.87	30.1	100.0	0.883
7	1.48	1.90	28.5	100.0	0.834
8	1.47	1.89	28.5	99.8	0.839
9	1.46	1.86	27.9	95.9	0.856
10	1.47	1.88	28.4	98.9	0.844
11	1.41	1.84	30.0	96.7	0.914
12	1.47	1.89	28.6	99.2	0.847
13	1.42	1.84	29.1	94.6	0.902
14	1.47	1.88	28.3	97.7	0.849
15	1.43	1.86	29.9	98.3	0.896
16	1.42	1.85	30.6	98.1	0.917
17	1.43	1.87	31.0	100.0	0.894
18	1.43	1.86	30.3	99.4	0.897
19	1.42	1.84	30.1	97.1	0.913
20	1.42	1.84	30.0	96.8	0.913
21	1.42	1.85	29.6	97.2	0.895
22	1.45	1.87	29.0	98.1	0.872
23	1.41	1.85	31.3	99.9	0.924
24	1.42	1.87	31.3	100.0	0.902
25	1.43	1.85	29.4	97.1	0.892
26	1.45	1.86	28.8	97.0	0.873
27	1.39	1.83	31.5	97.6	0.951
28	1.43	1.85	28.9	96.2	0.886
29	1.42	1.83	29.5	95.3	0.911
30	1.38	1.83	32.9	100.0	0.966
31	1.43	1.85	29.2	94.7	0.914

Table II (cont'd). Fairbanks silt specimen data for tension tests.

Test	Dry density (g/cm^3)	Wet density (g/cm^3)	Water content (%)	Degree of saturation (%)	Void ratio
32	1.42	1.84	29.5	94.5	0.925
33	1.45	1.86	28.1	93.1	0.892
34	1.45	1.86	28.3	93.5	0.894
35	1.44	1.88	30.4	99.7	0.901
36	M*	M	29.5	M	M
37	M	M	29.5	M	M
38	1.44	1.86	28.6	94.2	0.896
39	1.44	1.85	28.6	91.8	0.901
40	1.45	1.87	28.8	93.4	0.892
41	1.43	1.86	29.9	94.6	0.915
42	1.42	1.84	29.3	93.5	0.932
43	1.47	1.91	29.4	100.0	0.857
44	1.40	1.83	30.7	95.1	0.957
45	M	M	29.5	M	M
46	1.42	1.83	29.1	90.6	0.931
47	1.42	1.83	29.3	90.8	0.935
48	1.44	1.85	28.5	91.2	0.904
49	1.43	1.83	28.2	89.2	0.915
50	1.51	1.92	26.7	99.0	0.791
51	1.49	1.90	27.2	98.1	0.815
52	1.46	1.86	27.2	93.8	0.852
53	1.47	1.88	27.7	95.2	0.863
54	1.47	1.88	27.9	95.2	0.869

** M — data missing.*

the loss of soil during the air evacuation and saturation phase. A network of plastic tubing led from the four top adapters to a vacuum pump, and another network of tubing connected the four bottom adapters to a deaerated distilled water tank. A differential pressure between the air vacuum and the water tank vacuum was maintained so that the water would saturate the sample at a slow, steady rate. This pressure differential was found to be best at 30 ± 5 cm of Hg. Fast saturation rates were avoided because they could result in: 1) piping of the water through channels up along the outside circumference of the sample, 2) transverse breaking of the soil which could lead to harmful ice lenses upon freezing of the soil, and 3) incomplete evacuation of air. Approximately four hours was sufficient time to allow the samples to saturate.

The mold with the four samples was then placed in a 46- x 46- x 7-cm cold chamber and frozen for a minimum of 20 hours. The temperature in the chamber decreased very rapidly after the freezing process was initiated and reached -19°C after 10 minutes. At the end of 20 hours the temperature in the chamber was recorded at -37°C. The samples were frozen from the top down by placing combined Styrofoam and cork insulation under and around the mold, leaving the top metal end caps exposed to the freezing temperatures. During freezing, water was supplied to the samples through the bottom end caps to compensate for the upward migration of moisture. In this manner a uniform moisture content was achieved throughout the samples.

After the samples had completely frozen, the mold was removed from the cold chamber and placed in a coldroom at -7°C. The mold was conditioned at this temperature for a period of two to four hours to facilitate removal of the samples from the mold. The plastic inserts were removed from the samples and they were measured with a comparator for signs of eccentricity. Upon one complete revolution on the comparator, a sample with more than a 0.02-cm deflection was not accepted for testing. This corresponds to an error of 3% in the measured strength due

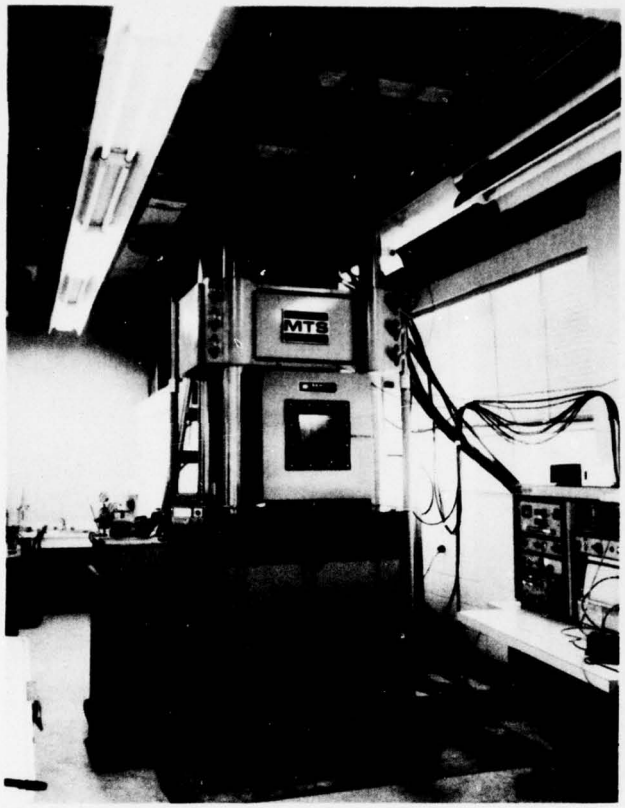

Figure 1. MTS testing machine and Bemco environmental chamber.

to a bending stress. A thin, flexible rubber membrane was then placed over the sample to protect it from sublimation. If it was not to be tested immediately, the sample was sealed in a plastic bag and stored in the -7°C coldroom until testing, for a period not exceeding two weeks.

APPARATUS AND TESTING PROCEDURE

Both the apparatus and the procedure for testing the frozen soil samples were very similar to those used in the strain rate effect investigation (Haynes et al. 1975).

All tests were performed using an MTS closed-loop electrohydraulic testing machine, Model 907.52, equipped with a temperature-controlled Bemco environmental chamber, shown in Figure 1. Because temperature was the important parameter in this investigation, a thermocouple was mounted adjacent to the sample to monitor the temperature in the chamber. To ensure against partial thawing of samples, tests at 0°C prompted the use of a heat sink device which would absorb the heat induced into the chamber every time the door was opened. The heat sink consisted of 16 one-gallon metal cans filled with crushed ice and placed around the sample in the chamber. This is shown in Figure 2.

Since the samples were stored in a coldroom at -7°C prior to testing, and were tested over a temperature range of -56.7°C to 0°C, sufficient time was allowed for the samples to reach an equilibrium state with the desired testing temperature of the chamber. From observations based on a dummy sample wired with eight thermocouples, it was found that a minimum conditioning time of 1½ hours was required for a test at -56.7°C, while the conditioning time for tests at other temperatures was usually not more than 1 hour.

Observations were also made on the internal temperature fluctuations of the environmental chamber and the temperature fluctuations initiated by the opening and closing of the chamber door. When the chamber remained closed, the temperature within the chamber cycled through a change of 0.8°C approximately every minute. This means that the temperature cycled between -0.4°C and +0.4°C for a test run at 0°C. Short-term fluctuations, e.g., about 3°C in 15 sec,

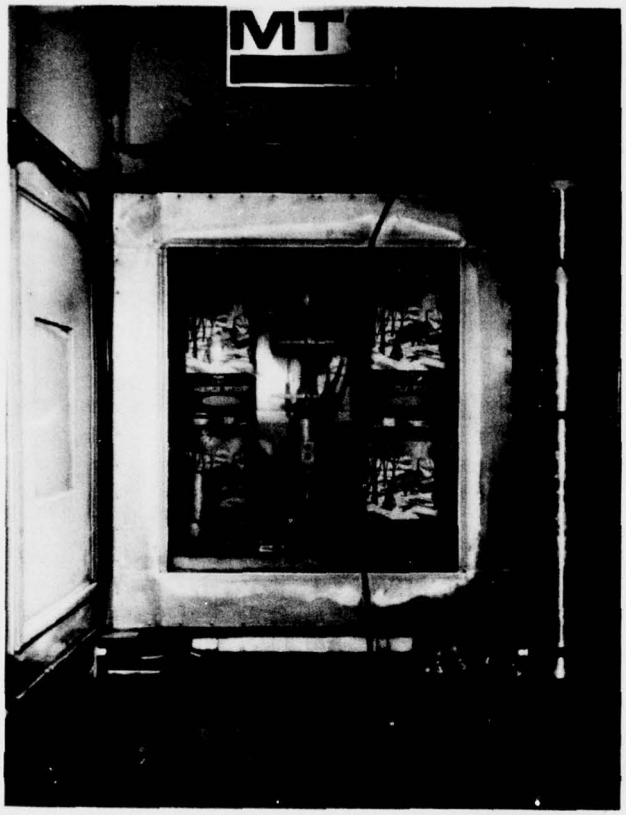

Figure 2. Sample in the environmental chamber with metal cans full of crushed ice used as a heat sink.

occurred when the chamber door was opened and then closed. The refrigeration system reacted quickly when it sensed the warmer air being drawn into the chamber as the door was closed, and worked continuously until the temperature was brought back to its desired value. The ice-filled metal cans helped significantly to stabilize the temperature and decrease the fluctuations.

The majority of samples were tested with a 25-metric-ton-capacity load cell, MTS Model 661.22, having an accuracy of ± 2% of the measured value. With lower expected loads at higher temperatures, and with slower loading rates, a more sensitive load cell was required; thus a 1-ton Baldwin-Lima-Hamilton SR-4 load cell was used for these test conditions.

Two linear variable differential transformer (LVDT) transducers were used to measure the axial deformation of the samples. They were attached to the sample end caps 180° apart, and their output signals were averaged to obtain the average displacement.

For all tests, load and displacement curves were recorded on a Tektronix dual-beam oscilloscope, Model R5103N. Load and time curves were recorded on a Tektronix dual-beam oscilloscope, Type 502A, with a Biomation transient recorder, Model 802. The fastest test had a time to failure of about 15 msec and, since this would have surpassed the response capacity of the MTS console strip chart recorder, the more responsive Biomation recorder was used.

Additional information concerning the apparatus and testing procedure can be obtained from the previous investigation (Haynes et al. 1975).

TEST RESULTS

Data for the uniaxial compression and tension tests are presented in Tables III and IV. A total of 108 tests were performed, 54 in tension and 54 in compression. Temperature was selected to be the principal variable in this investigation, and therefore tests were run at 0, -1.7, -5.6, -9.4, -17.8, -34.4, and -56.7°C. The lowest temperature capability of the Bemco refrigeration unit is -56.7°C, but at times this temperature could not be steadily maintained, and thus some tests had to be run at a higher temperature. The machine speed was operated in a constant displacement mode. Two rates of loading were used, 0.0423 cm/sec and 4.23 cm/sec, representing a slow-speed and a fast-speed test.

Table III. Compression test results for Fairbanks silt.

Test	Machine speed (cm/sec)	Temp (°C)	Strength (MN/m^2)	Strain	Strain rate ($sec^{-1} \times 10^{-2}$)	Time to failure (sec)	Initial tangent modulus (GN/m^2)	50% strength modulus (GN/m^2)
1	4.23	- 9.4	21.1	0.0092	38.18	0.024	8.3	3.3
2	4.23	- 5.6	14.5	0.0100	39.84	0.025	6.6	3.3
3	4.23	- 5.6	15.6	0.0100	43.30	0.023	6.6	3.0
4	4.23	- 5.6	14.4	0.0088	39.84	0.022	6.6	2.6
5	0.0423	- 9.4	5.7	0.0044	0.37	1.19	5.5	1.7
6	0.0423	- 5.6	4.4	0.0044	0.38	1.15	6.3	1.1
7	0.0423	- 5.6	4.3	0.0052	M*	M	5.5	1.4
8	4.23	-17.8	33.8	0.0127	20.56	0.062	7.9	4.8
9	4.23	-17.8	33.8	0.0127	22.37	0.057	11.0	4.7
10	0.0423	-17.8	12.1	0.0094	0.46	2.02	11.0	2.5
11	0.0423	-17.8	12.3	0.0088	0.48	1.82	11.0	2.8
12	4.23	-17.8	29.8	0.0120	22.13	0.054	11.0	4.2
13	4.23	-17.8	33.7	0.0139	27.34	0.051	11.0	4.4
14	4.23	-34.4	M	M	M	M	13.2	8.5
15	4.23	-34.4	56.6	0.0124	34.31	0.036	12.1	7.7
16	4.23	-34.4	54.8	0.0120	41.21	0.029	14.1	7.0
17	0.0423	-34.4	24.9	0.0104	0.37	2.83	9.8	4.4
18	0.0423	-34.4	25.7	0.0120	0.48	2.50	11.0	4.4
19	0.0423	-34.4	24.4	0.0112	0.53	2.11	10.0	4.4
20	0.0423	-34.4	22.8	0.0104	0.46	2.25	11.0	3.5
21	0.0423	-34.4	25.9	0.0112	0.44	2.56	11.0	4.4
22	4.23	-52.8	79.9	0.0125	38.95	0.032	21.9	8.8
23	4.23	-52.8	84.2	0.0121	81.74	0.038	21.9	9.3
24	4.23	-51.1	75.6	0.0115	39.51	0.029	17.4	7.7
25	0.0423	-48.3	40.9	0.0129	0.47	2.76	12.2	6.2
26	0.0423	-43.3	35.3	0.0107	0.46	2.30	11.0	5.8
27	4.23	-34.4	44.9	0.0116	46.32	0.025	11.0	6.2
28	4.23	-34.4	52.8	0.0130	41.89	0.031	18.3	7.3
29	0.0423	- 5.6	4.7	0.0049	0.43	1.14	3.1	1.4
30	0.0423	- 1.7	2.1	0.0049	0.40	1.23	1.1	0.54
31	0.0423	- 1.7	2.7	0.0059	0.60	0.98	1.5	0.83
32	0.0423	- 1.7	2.9	0.0053	0.43	1.24	2.1	0.83
33	4.23	- 1.7	11.0	0.0123	36.06	0.034	2.4	2.1
34	4.23	- 1.7	10.6	0.0100	38.35	0.026	4.3	2.1
35	4.23	- 1.7	11.0	0.0119	45.58	0.026	4.3	2.1
36	4.23	0	6.0	M	M	M	1.0	0.69
37	4.23	0	6.5	M	M	M	0.83	0.54
38	4.23	0	5.3	M	M	M	0.42	0.35
39	4.23	0	6.2	0.0159	61.31	0.026	0.90	0.90
40	0.0423	0	1.9	0.0084	0.57	1.46	0.15	0.13
41	0.0423	0	1.3	0.0084	0.69	1.21	0.52	0.43
42	0.0423	0	1.6	0.0076	0.65	1.17	0.58	0.52
43	0.0423	0	1.5	0.0101	0.83	1.21	0.48	0.37
44	4.23	- 9.4	23.7	0.0098	40.94	0.024	M	M
45	4.23	- 9.4	21.1	M	M	0.025	M	M
46	0.0423	- 9.4	4.5	M	M	1.35	M	M

* M — data missing.

Table III (cont'd). Compression test results for Fairbanks silt.

Test	Machine speed (cm/sec)	Temp (°C)	Strength (MN/m^2)	Strain	Strain rate ($sec^{-1} \times 10^{-2}$)	Time to failure (sec)	Initial tangent modulus (GN/m^2)	50% strength modulus (GN/m^2)
47	0.0423	- 9.4	6.1	M*	M	M	M	M
48	0.0423	- 9.4	7.2	M	M	1.50	M	M
49	0.0423	-50.0	43.1	0.0132	M	M	8.0	8.0
50	0.0423	-53.9	53.2	0.0132	M	M	11.8	6.7
51	0.0423	-55.6	51.0	0.0132	1.28	1.03	20.1	7.7
52	0.0423	-17.8	14.8	0.0175	1.65	1.06	6.3	5.0
53	0.0423	- 9.4	6.4	0.0079	0.35	2.23	4.0	2.5
54	0.0423	- 9.4	6.1	0.0070	0.41	1.71	4.0	2.5

* M — data missing.

Table IV. Tension test results for Fairbanks silt.

Test	Machine speed (cm/sec)	Temp (°C)	Strength (MN/m^2)	Strain	Strain rate ($sec^{-1} \times 10^{-2}$)	Time to failure (sec)	Initial tangent modulus (GN/m^2)	50% strength modulus (GN/m^2)
1*	4.23	- 9.4	6.0	0.00088	4.38	0.020	8.3	4.4
2*	4.23	- 9.4	5.7	0.00076	3.78	0.020	M†	5.9
3*	4.23	- 5.6	4.7	0.00094	6.24	0.015	11.0	5.5
4*	4.23	- 5.6	5.0	0.00095	6.32	0.015	11.6	5.5
5	0.0423	- 9.4	5.2	0.0041	0.19	2.14	6.9	1.7
6	0.0423	- 9.4	6.2	0.0088	0.33	2.67	3.4	1.4
7*	4.23	-17.8	5.6	0.00068	3.39	0.020	11.0	11.0
8*	4.23	-17.8	6.6	0.00083	3.77	0.022	27.4	7.7
9*	4.23	-17.8	7.0	0.00072	M	M	24.4	9.4
10*	4.23	-17.8	4.8	0.00064	M	M	14.6	11.0
11*	0.0423	-17.8	6.5	0.0021	0.12	1.76	14.6	4.2
12*	0.0423	-17.8	6.3	0.00151	0.09	1.63	12.6	4.9
13	0.0423	- 9.4	6.2	0.0046	0.16	2.93	21.9	1.6
14	0.0423	- 5.6	4.5	0.0080	0.31	2.60	4.4	0.9
15	0.0423	-34.4	9.0	0.00106	0.05	2.06	19.1	9.8
16*	0.0423	-34.4	4.2	0.00035	0.03	1.12	12.6	12.6
17	0.0423	-34.4	7.7	0.00088	0.05	1.77	15.7	9.2
18	0.0423	-34.4	6.6	0.00068	0.04	1.84	12.6	10.8
19*	4.23	-34.4	5.0	0.00068	5.26	0.013	M	M
20*	4.23	-34.4	6.8	0.00060	2.74	0.022	14.6	12.5
21	4.23	-34.4	4.9	0.00052	3.07	0.017	14.6	10.9
22*	4.23	-56.7	5.4	M	M	0.018	M	M
23	4.23	-56.7	9.1	0.00067	3.73	0.022	15.5	14.6
24*	0.0423	-56.7	8.4	0.00058	M	M	16.8	15.5
25	0.0423	-56.7	8.8	0.00088	M	M	11.2	11.0
26	0.0423	-56.7	9.4	0.00088	0.03	2.75	13.4	13.4
27*	0.0423	-56.7	6.1	0.00044	0.05	0.90	14.1	14.1

* Broke at end cap.
† M — data missing.

Table IV (cont'd).

Test	Machine speed (cm/sec)	Temp (°C)	Strength (MN/m^2)	Strain	Strain rate ($sec^{-1} \times 10^{-2}$)	Time to failure (sec)	Initial tangent modulus (GN/m^2)	50% strength modulus (GN/m^2)
28*	0.0423	-56.7	6.9	0.00052	0.06	0.83	14.0	14.0
29*	4.23	-56.7	5.1	0.00036	2.78	0.013	14.6	14.6
30	4.23	-56.7	7.6	0.00052	3.73	0.014	14.4	14.4
31*	0.0423	- 5.6	4.8	0.0057	0.27	2.09	4.3	2.1
32	0.0423	- 5.6	4.9	0.0082	0.35	2.37	8.6	1.4
33	0.0423	- 1.7	2.6	0.0082	0.42	1.95	2.7	0.7
34*	0.0423	- 1.7	2.2	0.0051	0.34	1.51	1.1	0.6
35	0.0423	- 1.7	2.8	0.0114	0.41	2.80	2.1	1.1
36	4.23	- 1.7	3.3	0.00143	7.95	0.018	3.1	2.6
37	4.23	- 1.7	3.0	0.00147	8.65	0.017	2.4	2.4
38*	4.23	- 1.7	3.6	0.00163	7.78	0.021	2.3	2.3
39*	4.23	0	2.4	0.00184	10.82	0.017	1.4	1.4
40	4.23	0	2.0	0.00215	11.92	0.018	2.1	1.1
41	0.0423	0	1.0	0.0074	0.50	1.46	0.6	0.3
42*	0.0423	-17.8	6.6	0.00200	2.09	2.15	8.6	4.3
43*	4.23	-17.8	7.1	0.00082	3.55	0.023	11.9	8.6
44*	4.23	- 5.6	4.6	0.00102	4.44	0.023	8.6	3.9
45*	0.0423	0	1.0	0.0060	0.40	1.48	0.5	0.3
46	0.0423	0	1.4	0.0084	0.39	2.15	0.7	0.5
47*	4.23	0	1.8	0.00168	10.49	0.016	1.3	1.2
48*	4.23	0	1.9	0.00195	13.00	0.015	1.7	1.1
49	0.0423	0	1.1	0.0092	0.64	1.45	0.6	0.4
50	4.23	- 9.4	6.1	M†	M	M	M	M
51	4.23	- 9.4	5.5	M	M	M	M	M
52	0.0423	- 9.4	6.3	M	M	M	M	M
53*	4.23	- 9.4	5.6	0.00105	3.76	0.028	6.0	6.0
54	4.23	- 5.6	5.3	0.00132	4.70	0.028	8.0	4.0

** Broke at end cap.*

† M – data missing.

For compression tests at the slower machine speed, the time to failure was from 0.98 to 2.83 sec. The time to failure at the higher speed was from 22 to 62 msec. For tension tests at the slower rate of loading, the time to failure was from 0.83 to 2.93 sec. At the higher speeds the time to failure was from 13 to 28 msec.

At least three tests were run at each specified temperature for each machine speed in both tension and compression. If the results were not satisfactory, more tests were conducted. This approach applied especially to tension tests, since more than half of the samples broke at the end cap, which was not the desired plane of failure. Therefore, at each combination of temperature and machine speed, an attempt was made to run tests until at least one sample failed in the neck-down section of the dumbbell-shaped sample. An average value of strength at each temperature and machine speed was then computed and plotted on the various graphs.

Determination of the failure stress from the load-deformation curves for some compression tests conducted at low strain rates is discussed by Haynes et al. (1975). They conclude that the failure stress can be determined when the final tangent modulus begins on the load-deformation curve.

In the present study, failure stress or maximum stress is easily identifiable for all tension tests and for rapid compression tests at low temperatures. However, for the slow compression tests and for tests at

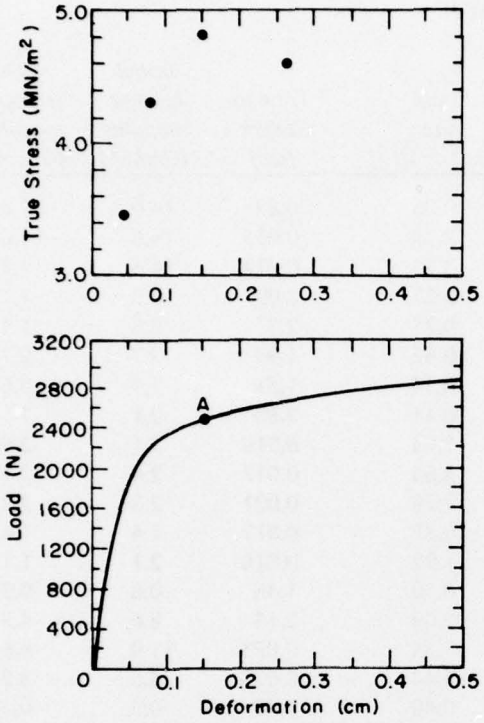

Figure 3. Typical load and true stress versus deformation for compression tests at slow speeds and temperatures above –18°C.

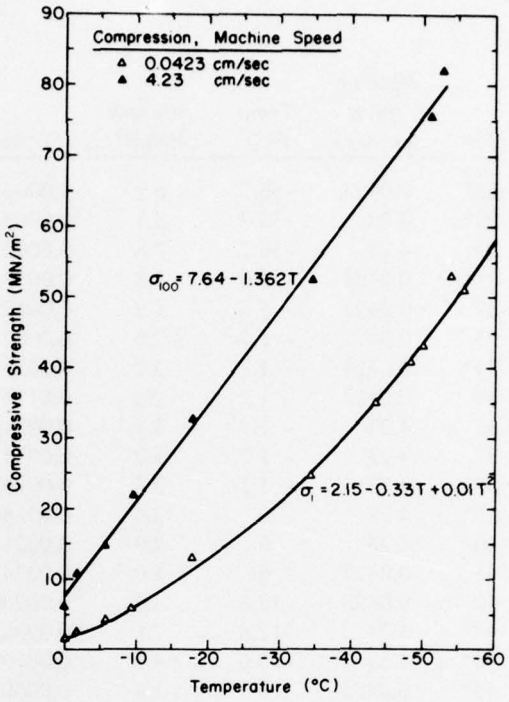

Figure 4. Average strength vs temperature for the compression tests.

temperatures above –18°C, the tangent modulus decreased until a final constant modulus was established for an increasing load. For example, point A in Figure 3 marks the onset of this final constant modulus for one of these tests. The true stress was found for a compression test by assuming a Poisson's ratio of ½ to account for the increase in cross-sectional area. The plot of true stress versus deformation in Figure 3 shows that the maximum true stress coincided with point A. Therefore, in this report, point A was selected as the point of failure stress for the high temperature and slow machine speed compression tests. Also, point A is easily determined for each load-deformation test record. An analysis was done by Haynes et al. (1975) to determine the strain in the neck section of a dumbbell specimen. A factor of 0.349 ΔL, where ΔL is the deformation measured by the LVDT's between end caps, was used for calculating the strain.

Figure 4 shows the relationship between the strength and temperature for the compression tests. At a machine speed of 4.23 cm/sec, the average strength increased from 6.0 MN/m² at 0°C to 82.1 MN/m² at –52.8°C. At a machine speed of 0.0423 cm/sec, the average strength increased from 1.6 MN/m² at 0°C to 53.2 MN/m² at –53.9°C.

The relationship between the tensile strength and temperature is shown in Figure 5. Each point plotted is an average of three or more tests. All tests, including those in which samples failed at the end caps, have been used for this graph. At least one specimen failed in the neck-down section of the sample for each combination of temperature and machine speed, except at –17.8°C and 4.23 cm/sec, for which all specimens failed at the end cap. The reason for specimen failure at the end cap is that unequal thermal contraction between the aluminum end cap and frozen soil produced strains in the frozen soil prior to testing.

The calculation of the failure stress for each test was based on the cross-sectional area of the neck section of the sample. The rationale for plotting all test results in Figure 5, including those where failure occurred at the end cap, is that this minimum area sustained the failure load even though it was not always the failure plane. The curves in Figure 5 therefore represent the minimum failure stress over the range of test temperatures. With a machine speed of

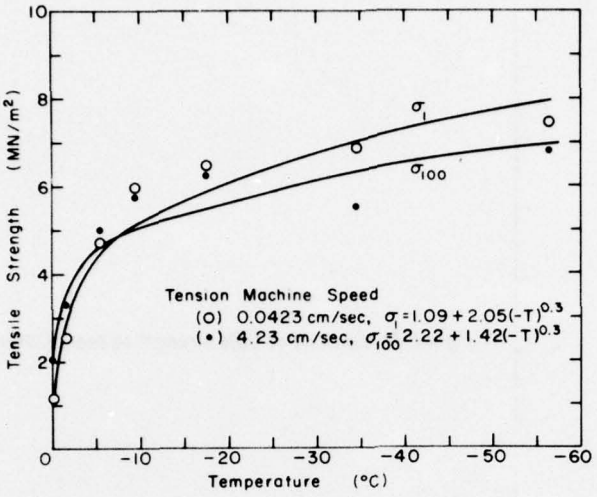

Figure 5. Average minimum strength vs temperature for the tensile strength tests.

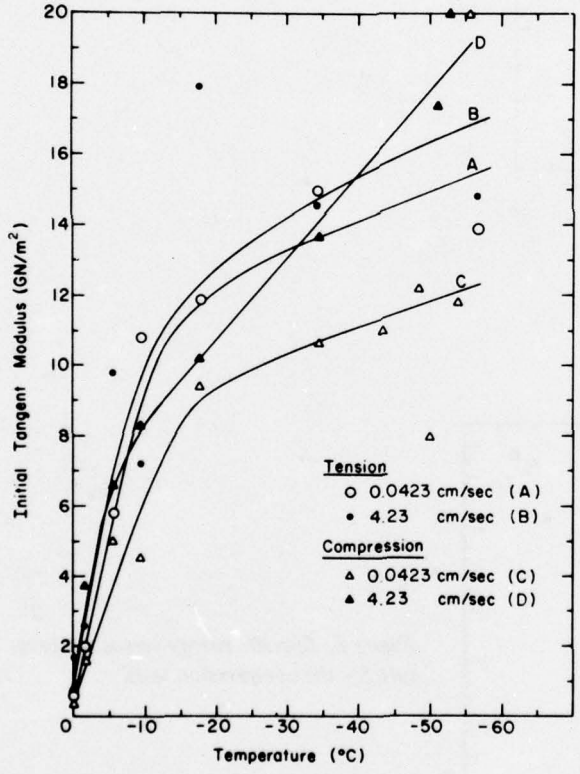

Figure 6. Initial tangent modulus vs temperature.

4.23 cm/sec, the average tensile strength increased from 2 MN/m² at 0°C to 6.8 MN/m² at -56.7°C. At a machine speed of 0.0423 cm/sec the average strength increased from 1.0 MN/m² at 0°C to 7.9 MN/m² at -56.7°C.

The correlation between the initial tangent modulus and temperature is shown in Figure 6. The relationship between the modulus at 50% strength and temperature is shown in Figure 7. In both graphs, the modulus increases with decreasing temperature. The largest rate of increase is at temperatures close to 0°C.

The specific energy for each test was found by computing the area under the stress-strain curve up to the failure stress. The areas were found by using an

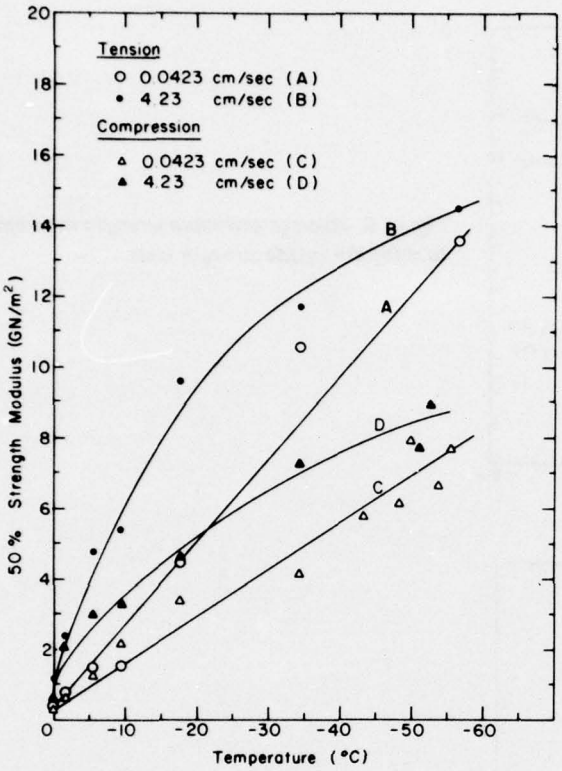

Figure 7. Modulus at 50% strength vs temperature.

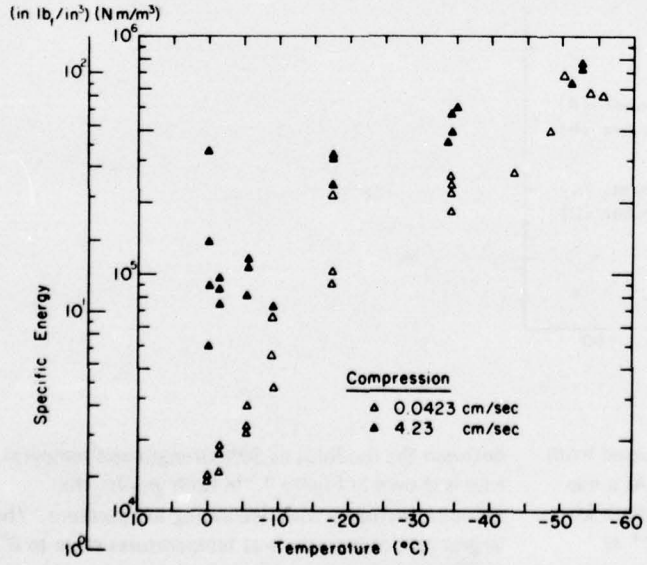

Figure 8. Specific energy versus temperature for the compression tests.

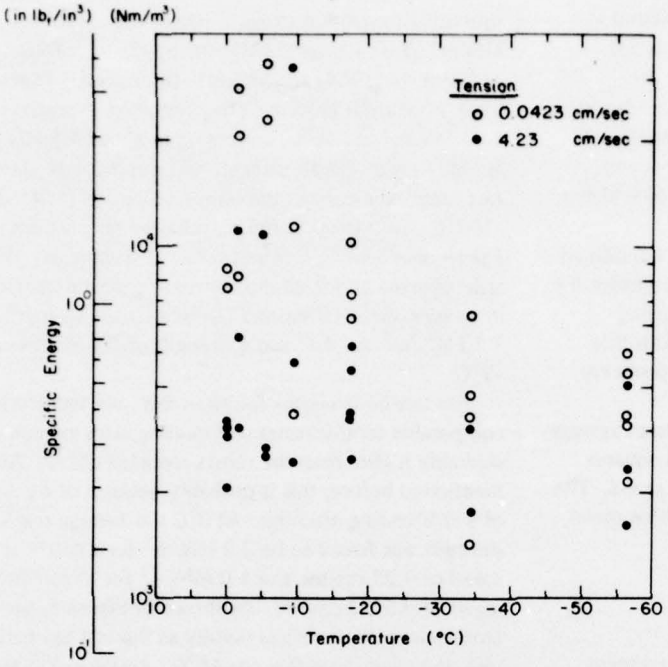

Figure 9. Specific energy versus temperature for the tension tests.

A-12 Antech planimeter with a 102-A Antech measurement scanning camera. The error involved in using this optical method of determining areas was about 1%.

Figures 8 and 9 show the relationship between specific energy and temperature for the compression and tension tests respectively. For the compression tests, the specific energy increased with decreasing temperature. The compressive tests with slower machine-speed show a greater change in specific energy over the temperature range than those with the faster machine-speed compression. For the tension tests, the specific energy decreased with decreasing temperature; and for the tests at the slower machine speed, the specific energy decreased more rapidly than for the tests run at the higher speed.

DISCUSSION

Compressive strength

Several investigators have tested frozen soil in uniaxial compression down to -195°C. Kaplar (1953) tested New Hampshire silt in uniaxial compression with a loading rate of 2.75 MN/m^2-min. At -24°C he found a maximum stress of 16.9 MN/m^2 and at -0.6°C a maximum stress of 2.1 MN/m^2. Wolfe and Thieme (1964) conducted tests on 2.54- x 2.54- x 5.08-cm parallelepipeds of silt and clay. At -60°C they found the compressive strength for silt to be about 29 MN/m^2 and at -10°C about 5.5 MN/m^2. The highest strength they obtained for silt was 75.8 MN/m^2 at -134°C. They do not report the applied loading rate.

Sayles (1966) tested frozen Ottawa sand down to -184°C. He conducted unconfined compression tests on cylinders 7.1 cm in diameter and 15.2 cm long. Using a machine speed of 0.51 cm/min he found maximum strengths of 37 MN/m^2, 41.8 MN/m^2 and 43 MN/m^2 at -41°C, -69°C, and -131°C respectively. Mellor and Smith (1966) tested frozen sand in the range of 0 to -35°C. With a machine speed of 14.66 cm/min, they found maximum rupture stress values of 2.3 MN/m^2, 4.9 MN/m^2 and 7.8 MN/m^2 at 0, -10, and -35°C respectively. Vialov (1965) conducted creep tests on frozen Callovian sandy loam with a time to failure of 10 min. He reports strengths of 4.2 MN/m^2, 6.9 MN/m^2 and 12.5 MN/m^2 at temperatures of -5, -10 and -20°C respectively.

The compressive strength found in this study was considerably greater than that found by other investigators with comparable soils at temperatures below -10°C. Tests conducted with a machine speed of 4.23 cm/sec produced strengths from 1.5 to 3 times as high as those run at 0.0423 cm/sec. These results are in good agreement with those found by Haynes et al. (1975). The strength of this soil can be expected to double when the machine speed is increased by two

orders of magnitude. The average strength found at 0°C with a machine speed of 4.23 cm/sec was 6.0 MN/m^2, and with a speed of 0.0423 cm/sec the average was 1.6 MN/m^2. These values are comparable to those reported by other investigators. The average strength found at -52.8°C was 82.1 MN/m^2 for the higher machine speed and this is typically 100% higher than other reported values.

In this study all tests were conducted on a relatively stiff machine. This machine prevents, to a considerable degree, energy stored in the system from causing specimen failure once cracks are initiated. It is this characteristic of the testing machine which probably produced the higher strength values.

Each point plotted on Figure 4 represents an average of three or more test values. Using the least squares method, a line was drawn for each machine speed. The equation obtained for the 4.23-cm/sec machine speed is

$$\sigma_{100} = 7.64 - 1.362T \quad (1)$$

where σ is the strength in MN/m^2, and T is temperature in °C. Unless otherwise noted, the subscripts 100 and 1 refer to the machine speed in inches per minute. The correlation of strength with temperature for the 0.0423-cm/sec machine speed was also developed with the method of least squares. It was found that the second-degree relationship was the best fit for the temperature range used in the tests. The equation obtained is

$$\sigma_1 = 2.15 - 0.33T + 0.01T^2 \quad (2)$$

where the symbols are the same as used above. Further testing at lower temperatures may show a higher order relationship between the strength and temperature.

Haynes (1976) showed that the uniaxial compressive strength of polycrystalline ice increases at a rate of about 0.7 MN/m^2-°C as temperature decreases. This effect strengthens the ice matrix in the frozen soil. Equation 1 predicts that the soil strength would increase at the rate of 1.362 MN/m^2-°C. Strengthening of the ice matrix accounts for about half of the rate increase predicted by eq 1. The other half is accounted for by other factors such as the quantity of unfrozen water discussed later in this report, and friction between grains of silt and/or ice discussed by Sayles (1973). These same factors will be involved in the increase in strength predicted by eq 2.

Tensile strength

Kaplar (1953) conducted direct tension tests on New Hampshire silt with cylindrical specimens. He found the maximum stress to increase from 0.34 MN/m^2 at -0.3°C to 5.2 MN/m^2 at -24°C. Wolfe and Thieme (1964) tested briquette-shaped silt specimens in uniaxial tension. They reported strengths of 1.03 MN/m^2 at -10°C, increasing to about 4.5 MN/m^2 at -80°C. The tensile strength did not increase above this value even though the temperature was lowered to -195°C. Offensend (1966) conducted tensile tests on Fairbanks silt using briquette-shaped specimens. He also reported an increase of strength with a decrease in temperature. Offensend found a tensile strength of 1.72 MN/m^2 at -4°C and a strength of 2.4 MN/m^2 at -9°C.

The tensile strengths found in this investigation at comparable temperatures and loading rates are considerably higher than the values reported above. As mentioned before, this is probably because of the use of a stiff testing machine. At 0°C the average tensile strength was found to be 2.0 MN/m^2 for a machine speed of 4.23 cm/sec and 1.0 MN/m^2 for a machine speed of 0.0423 cm/sec. As shown in Figure 5, the tensile strength increased rapidly as the test temperature decreased from 0°C to -10°C. Below -10°C the tensile strength continued to increase but at a reduced rate. The tensile strength was lower at 0°C for the slower machine speed but this effect reversed for temperatures below -10°C. Haynes et al. (1975) found the tensile strength of Fairbanks silt to be relatively insensitive to strain rate and the results of this investigation show some agreement with that finding.

Figure 5 shows the plot of the average maximum tensile stress values at each test temperature. The least squares method was used to obtain the following correlating equations:

$$\sigma_{100} = 2.22 + 1.42\,(-T)^{0.3} \quad (3)$$

$$\sigma_1 = 1.09 + 2.05\,(-T)^{0.3} \quad (4)$$

where σ_{100} and σ_1 are the maximum stresses in MN/m^2 at machine speeds of 4.23 cm/sec and 0.0423 cm/sec respectively.

The tensile strength increases rapidly, about 0.4 MN/m^2-°C, as the test temperature decreases from 0 to -10°C. Below -10°C the strength increases at a rate of about 0.04 MN/m^2-°C. Internal structural changes in ice around -10°C are reported by Butkovitch (1954) and Dillon and Andersland (1967). These changes may explain the rate change in strength observed in Figure 5. The strengthening of the ice matrix discussed earlier and the decrease in unfrozen water discussed later in this report may also explain the increase in tensile strength with decreasing temperature.

Initial tangent and 50% stress moduli

The modulus of elasticity was determined by Kaplar (1963) using a dynamic method of longitudinal vibrations. He found the modulus to increase from 1.17×10^{10} N/m^2 at 0°C to 2.27×10^{10} N/m^2 at -23°C for Fairbanks silt. Offensend (1966) found from tension tests the modulus for Fairbanks silt to be 4.7×10^{9} N/m^2 at -4°C with a machine speed of 2.54 cm/min. At -9.4°C he determined the modulus to be 1.19×10^{10} N/m^2. For polycrystalline ice tested at -7°C, Hawkes and Mellor (1972) reported modulus values from compression tests ranging from 5.8×10^{9} N/m^2 to 1.1×10^{10} N/m^2, and from tension tests from 4.1×10^{9} N/m^2 to 6.8×10^{9} N/m^2.

The initial tangent modulus results of this study are shown in Figure 6. At comparable temperatures, they are lower than the values found by Kaplar (1963). This result might be expected since Kaplar's method employed much lower strains. The tests in this study with the higher machine speeds, and consequently lower strains, produced the highest modulus. The modulus results of this study are slightly higher than those found by Offensend and show good agreement with the modulus for ice reported by Hawkes and Mellor (1972) at comparable strain rates and temperatures. The modulus values at 50% strength are slightly lower than the initial tangent modulus and are shown in Figure 7. Also, the tension tests produced consistently higher modulus values than the compression tests and the higher machine speed tests produced higher values for both tension and compression tests.

Specific energy

During a uniaxial test, tensile cracks are produced in a material. These cracks cause separation of the material in a tensile test and splitting and possible separation in a compression test. In this investigation, the specific energy was based upon the maximum stress. Separation was not observed when the maximum stress occurred for compression and tension tests conducted at 0°C and at the lower machine speed. The effect of strain rate on specific energy for frozen materials is discussed by Sayles and Epanchin (1966), Fairhurst (1970), Hawkes and Mellor (1972) and Haynes et al. (1975). There is general agreement that, with an increase in strain rate, the specific energy tends to increase slightly in compression tests and to decrease in tension tests.

The effect of temperature on the specific energy for Ottawa sand was determined in compression tests by Sayles and Epanchin (1966). At -3°C they found the energy to range from 3.4×10^{4} to 4.2×10^{4} N-m/m^3. When the test temperature was lowered to -30°C, the energy increased to the range of 9.8×10^{4} to 14.3×10^{4} N-m/m^3.

The specific energy results for this investigation are shown in Figures 8 and 9. The specific energy found in this study is about the same as Sayles and Epanchin (1966) report at -3°C, but slightly higher than their value at -30°C. For the compression tests, the energy increases about an order of magnitude for the high-speed tests and about 1.5 orders of magnitude for the low-speed tests as the temperature is lowered from 0 to -56.7°C. It should be noted that the specific energy for tests with a lower machine speed increased more rapidly than it did for the tests with the higher machine speed, although the latter had the higher energy values.

A general decrease in specific energy with lower temperatures for the tension test is shown in Figure 9. Unlike the compression test results, the lower machine speed produced the higher energies for the tensile tests. However, one similarity with the compression test results is that the specific energy may be insensitive to machine speed at temperatures below -60°C, even though the values are much lower than those at higher temperatures.

Mode of failure

The modes of failure encountered with uniaxial tests on frozen soil, ice, and rocks are described by Hawkes and Mellor (1970, 1972) and Fairhurst (1970). In general, brittle fracture characterizes elastic behavior, while ductile fracture characterizes some degree of plastic deformation. A brittle fracture criterion that has gained wide acceptance is that proposed by Griffith (1924). His assumption of crack growth from flaws in a material appears reasonable, since it is known that flaws such as bubbles, cracks and grain boundaries exist in ice and frozen soil. Griffith's biaxial failure criterion may be stated as:

$$\sigma_1 \geq K \text{ when } 3\sigma_1 + \sigma_2 \geq 0$$

$$(\sigma_1 - \sigma_2)^2 + 8K(\sigma_1 + \sigma_2) = 0 \text{ when } 3\sigma_1 + \sigma_2 \leq 0$$

where σ_1 and σ_2 are principal stresses and K is a function of the material properties and the crack geometry. Griffith's assumption that only tensile stresses are permitted on the boundary of a discontinuity is questionable, as is his conclusion that the compressive strength of a brittle material is eight times the tensile strength. A modification of Griffith's theory by McClintock and Walsh (1963) partially overcomes the restriction of a fixed ratio of compressive to tensile strength.

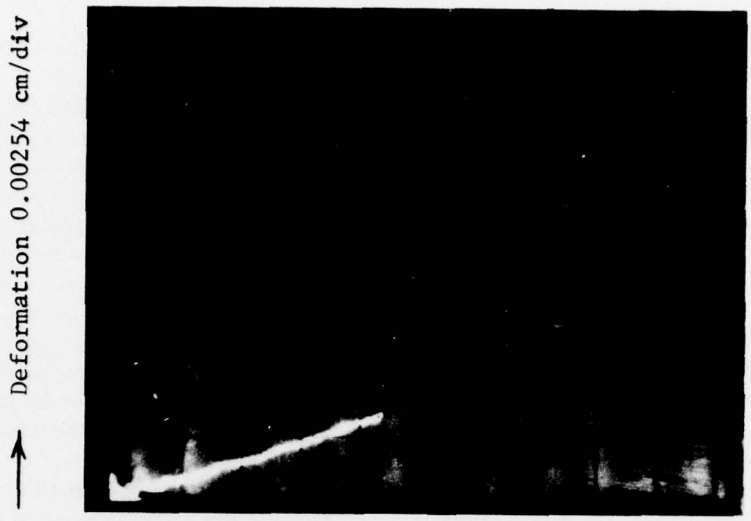

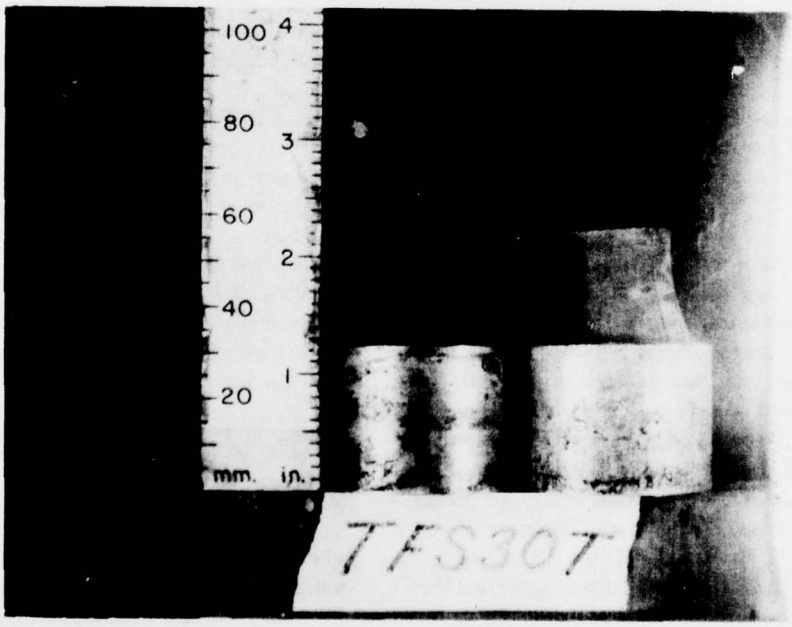

Figure 10. Tensile test at -56.7°C with a machine speed of 4.23 cm/sec.

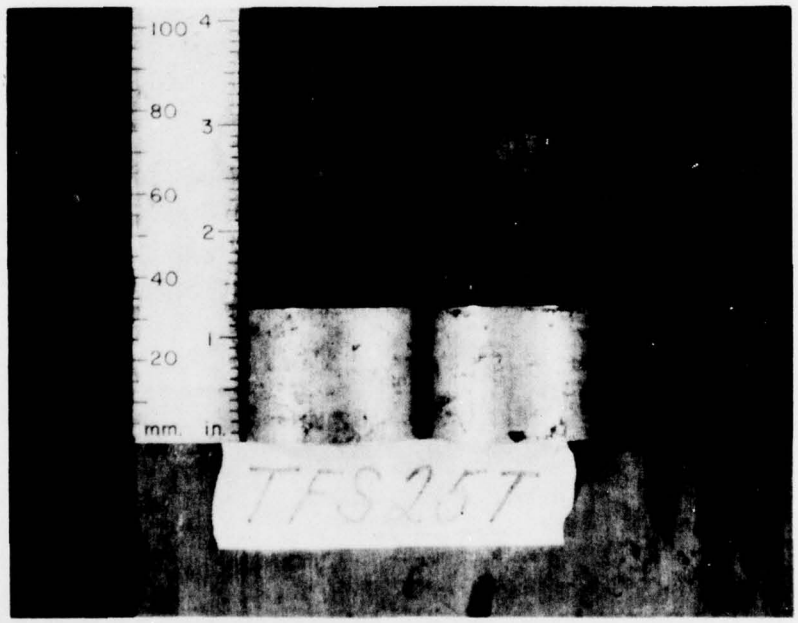

Figure 11. Tensile test at -56.7°C with machine speed of 0.0423 cm/sec.

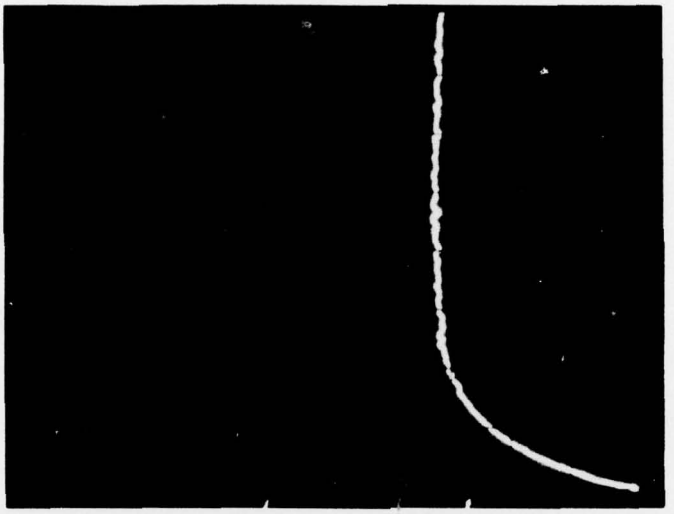

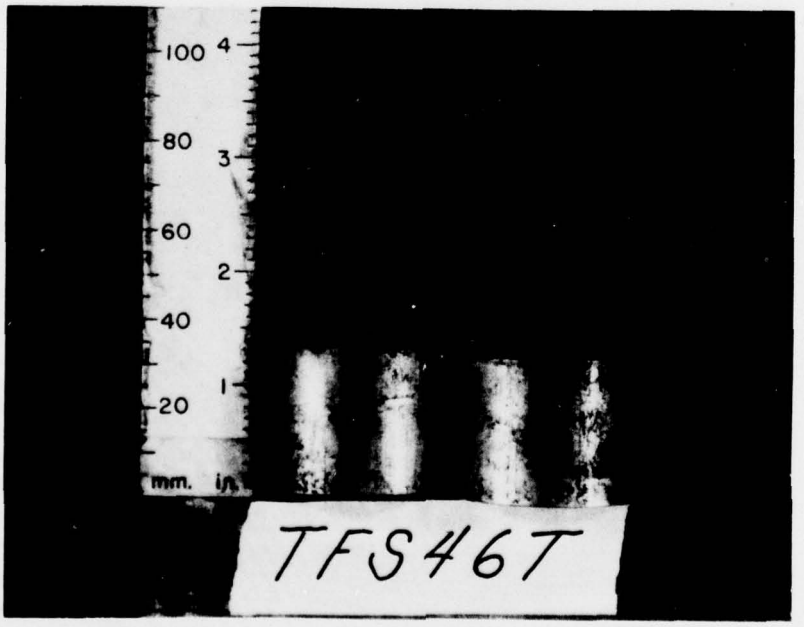

Figure 12. Tensile test at 0° C with a machine speed of 0.0423 cm/sec.

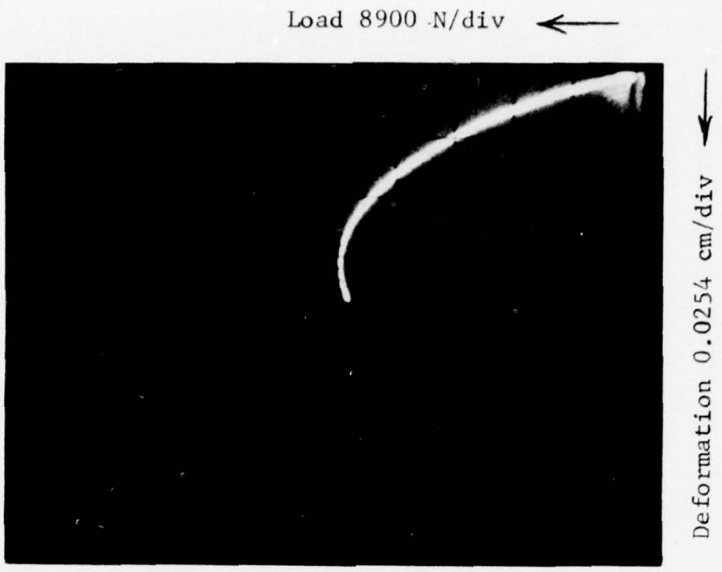

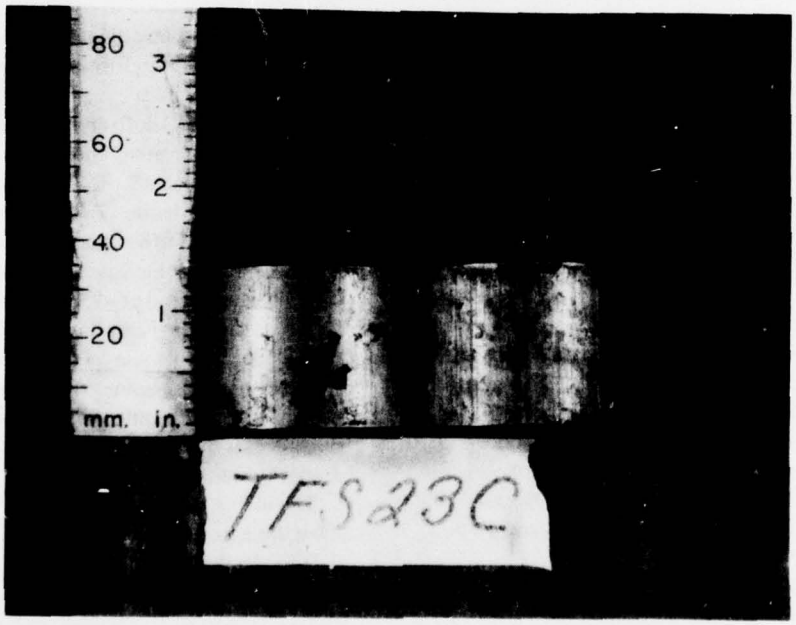

Figure 13. Compression test at -53°C with a machine speed of 4.23 cm/sec.

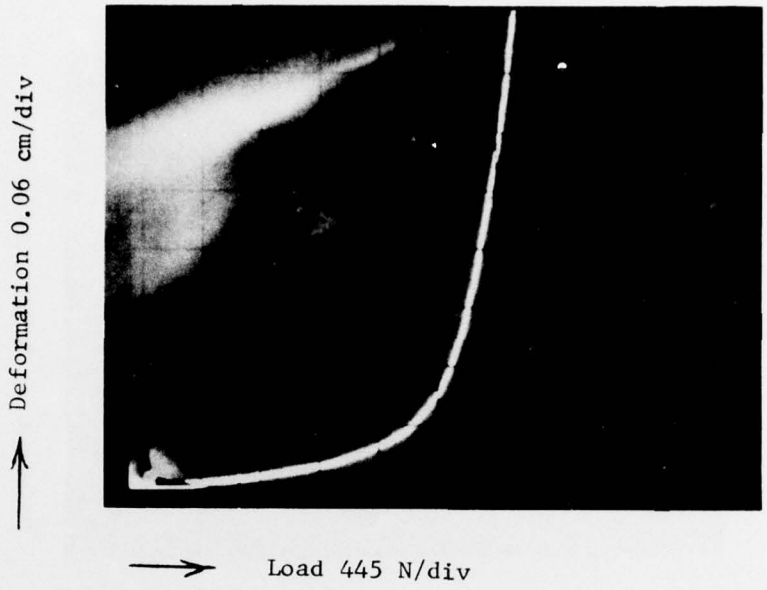

Figure 14. Compression test at 0°C with a machine speed of 4.23 cm/sec. (See cover for photograph of sample.)

In this investigation, all tensile tests exhibited a brittle fracture (see Fig. 10–12). The fracture plane for the tensile tests was often irregular. This result is discussed by Hawkes and Mellor (1970) and Peng (1975). They describe a tensile test in which cracks may initiate and then be arrested at several different locations on the ultimate failure surface. As the load increases, these cracks coalesce until the sample breaks. The resulting fracture surface may not be a plane because the individual cracks are seldom coplanar.

For the compression tests, a brittle fracture was observed at lower temperatures with the 4.23 cm/sec machine speed as shown in Figure 13. At higher temperatures and at the 4.23-cm/sec machine speed, Figure 14 shows that a combination of ductile and brittle fracture was found; also see cover photograph. At a machine speed of 0.0423 cm/sec, a ductile failure such as the failures shown in Figures 15 and 16 was observed at all temperatures.

The ratio of uniaxial compressive strength to uniaxial tensile strength found in this study varies widely with temperature and strain rate; e.g., the ratio ranges from 12 to 1 at -56°C to 3 to 1 at -30°C. Although Griffith's failure-by-flaw concept is probably applicable to brittle fracture in soils, the fixed ratio of uniaxial strengths demanded by his criterion is not supported by the data.

Strength as a function of unfrozen water

Mellor (1971) investigated the uniaxial compressive and tensile strengths for various rocks as a function of water content. At -25°C, the compressive strength of Berea sandstone and Indiana limestone decreased as the water content was increased from 0 to 1.0×10^{-3} g water/g rock, then it increased with higher water contents. A similar result was obtained for Barre granite. The uniaxial tensile strength for Indiana limestone increased with an increase in water content when tested at -25°C. The tensile strength for Berea sandstone and Barre granite exhibited little change with an increase in water content when tested at -25°C. Mellor assumes that the absorbed water remains essentially unfrozen for low water contents. He discusses theories which may explain the observed strength results.

The unfrozen water content was calculated by using the equation $W_u = \alpha\theta^{\beta}$ given by Tice et al. (1973). In this power equation, θ is the temperature in °C below freezing and α and β are empirical constants characteristic of a given soil. Figure 17 shows that the uniaxial compressive strength for Fairbanks silt decreases considerably as the unfrozen water content increases from 0.013 to 0.05 g water/g dry soil. The following equations were found using a least squares regression fit to the data:

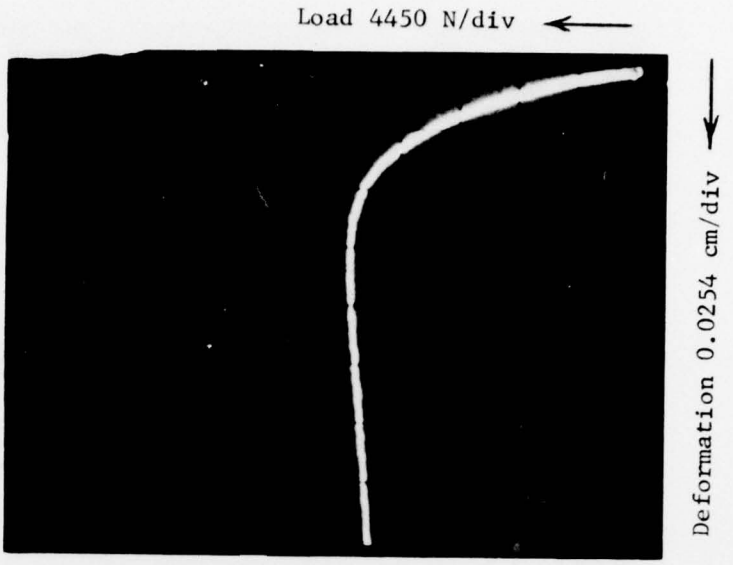

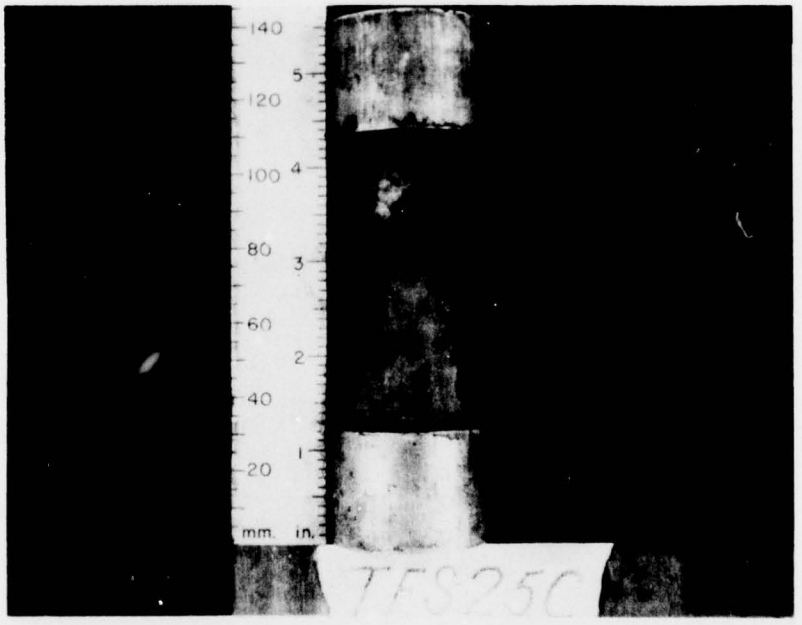

Figure 15. Compression test at -48°C with a machine speed of 0.0423 cm/sec.

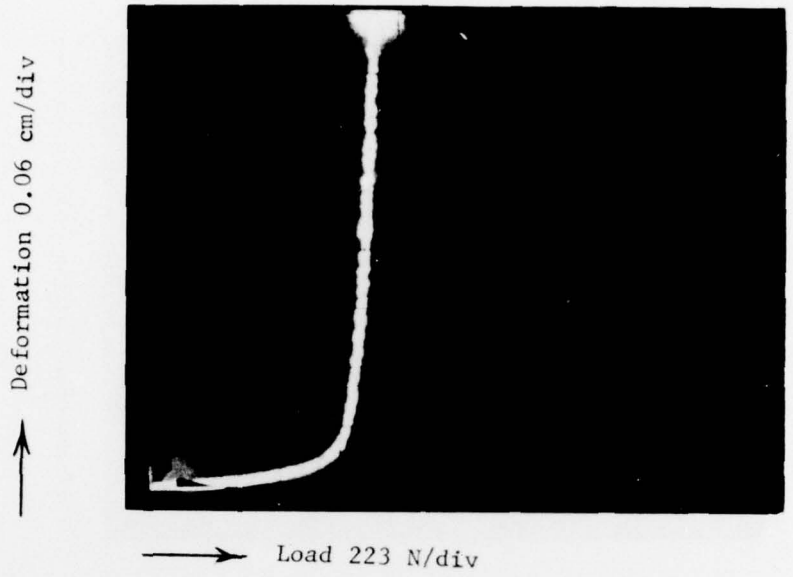

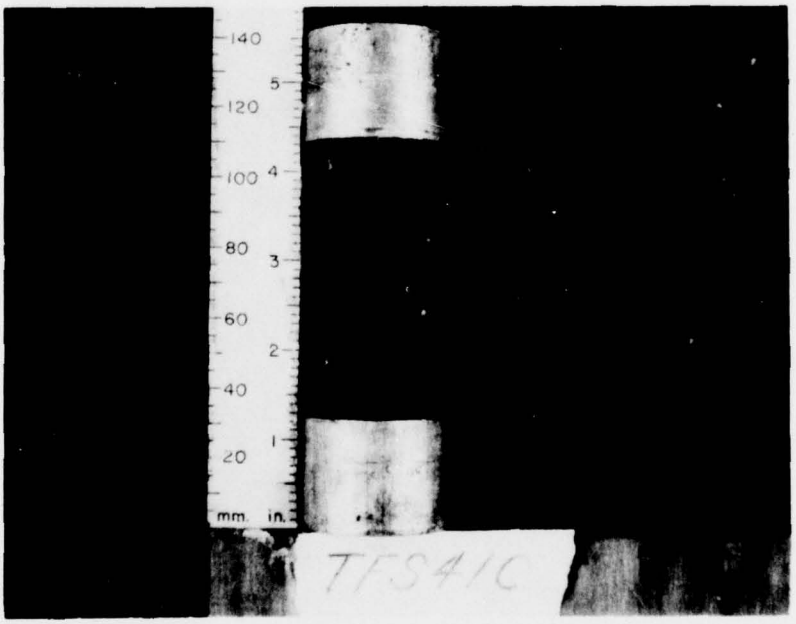

Figure 16. Compression test at 0°C with a machine speed of 0.0423 cm/sec.

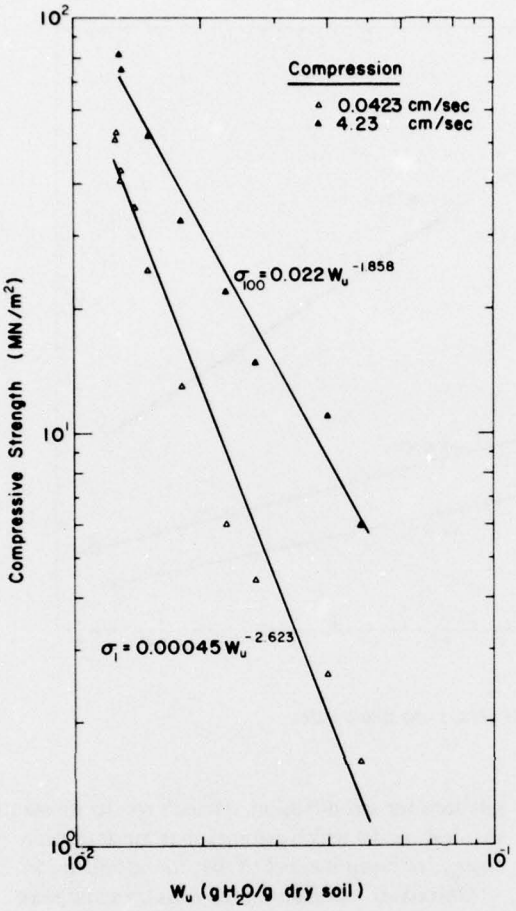

Figure 17. Correlation of uniaxial compressive strength and unfrozen water content.

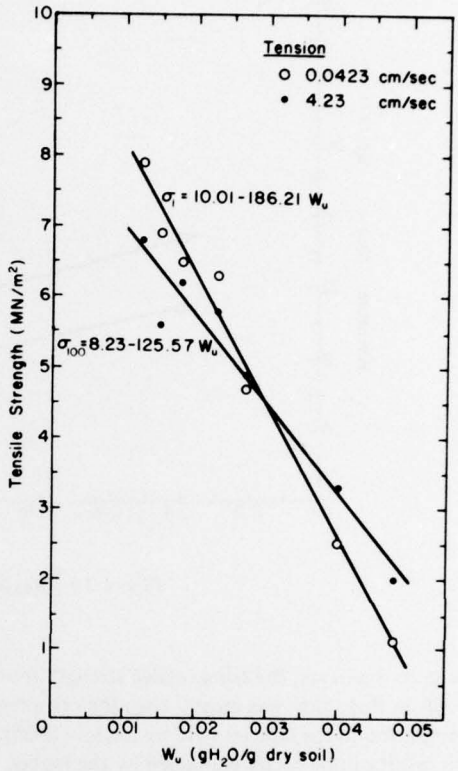

Figure 18. Correlation of uniaxial tensile strength and unfrozen water content.

$$\sigma_{100} = 0.022 W_u^{-1.858} \quad (5)$$

$$\sigma_1 = 0.00045 W_u^{-2.623} \quad (6)$$

where σ_{100} and σ_1 are the strengths in MN/m^2 for machine speeds of 4.23 cm/sec and 0.0423 cm/sec respectively, and W_u is the unfrozen water content in g water/g dry soil.

Figure 18 shows the relationship between uniaxial tensile strength and unfrozen water content. The strength decreases appreciably as the unfrozen water content increases from 0.012 to 0.048 g water/g dry soil. A least squares fit to the data produced the following equations:

$$\sigma_{100} = 8.23 - 125.57 W_u \quad (7)$$

$$\sigma_1 = 10.01 - 186.21 W_u \quad (8)$$

where the notation is the same as that given above. However, extrapolation with the expressions given above may not be valid beyond the range of the plotted test results.

The dependence of the strength of frozen soils on the quantity of unfrozen water is discussed by Sayles (1966) and Sayles and Haines (1974). They point out that the soil particle size, shape and consequent specific surface area affect the unfrozen water content and strength. For example, Ottawa sand has a large particle size, a low specific surface area, a low unfrozen water content, and a high strength. By comparison, a silt has a smaller particle size, a higher specific surface area, a higher unfrozen water content at comparable temperatures, and a lower strength. The results of this study do agree with this explanation with respect to the unfrozen water content; e.g., a lower unfrozen water content produces a higher

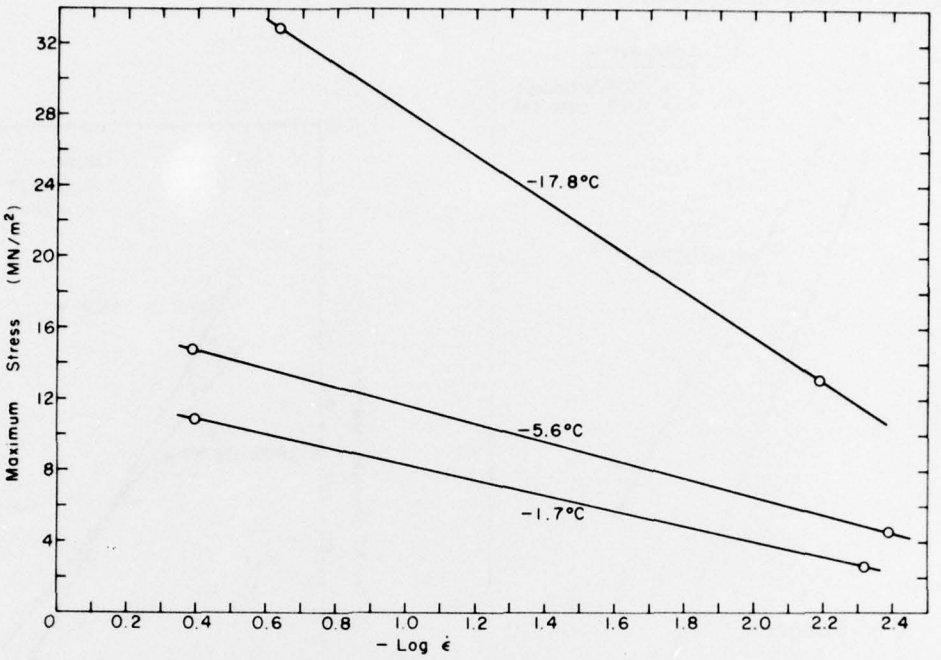

Figure 19. Maximum stress versus log strain rate.

strength. However, the compressive strength found for silt in this study was greater than the compressive strength found for Ottawa sand by Sayles (1966). This result can be partly explained by the higher machine speed used in this study, 0.0423 cm/sec, compared with that used by Sayles, 0.008 cm/sec.

Thermal activation

A failure mechanism based on thermal activation to cause dislocation has been used successfully to explain creep behavior in many materials. Mellor (1971) discusses such a mechanism with respect to the failure of various rocks at temperatures from +23°C to −195°C. He obtained activation energy values ranging from 0.38 to 0.51 kcal/mol (1.59×10^3 to 2.13×10^3 J/mol). Kumar (1968) also obtained the activation energy for rocks over the same temperature range. He concluded that the fracture mechanisms for basalt and granite were thermally activated. Activation energy values of 0.45 kcal/mol (1.88×10^3 J/mol) for basalt and 0.34 kcal/mol (1.42×10^3 J/mol) for granite are reported by Kumar. Heard (1963) reports activation energy values of 45.7 to 62.4 kcal/mol (1.91×10^5 to 2.6×10^5 J/mol) for marble based on confined creep tests made at 400°C to 500°C. Mellor points out that the activation energy for typical rocks is about 60 kcal/mol (2.5×10^5 J/mol) as calculated from expirical relations for self-diffusion. Heard's results substantiate the flow model which assumes that the activation energy for creep is equal to that for self-diffusion.

Uniaxial compression creep tests on snow were conducted by Landauer (1955). From these tests made at −5°C, −10°C, and −20°C, he found an activation energy of 14 kcal/mol (5.86×10^4 J/mol). The relationship between creep rate and temperature was investigated by Glen (1958). He performed creep tests on ice at temperatures from −0.02°C to −12.8°C and obtained a value of 31.8 kcal/mol (1.33×10^5 J/mol) for the activation energy. Dillon and Andersland (1967) conducted creep tests on polycrystalline ice over a temperature range of −1.5°C to −10°C. They report an activation energy of 11.4 kcal/mol (4.77×10^4 J/mol). They also observed higher activation energies for higher stresses and warmer temperatures. From their creep data there appears to be some internal structural change in ice at temperatures around −10°C.

In this study, the method of calculating the activation energy is similar to that used by Heard (1963). The general form of the Arrhenius equation for thermally activated creep is

$$\dot{\epsilon} = \dot{\epsilon}_0 \exp(-E/RT) \sinh(\sigma/\sigma_0) \qquad (9)$$

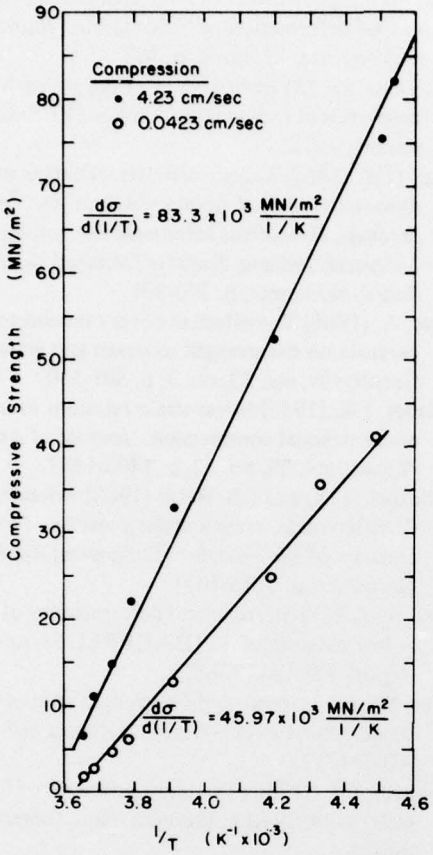

Figure 20. Compressive strength versus reciprocal of absolute temperature.

where $\dot{\epsilon}$ = strain rate
$\dot{\epsilon}_0$ = constant with dimensions of strain rate
E = activation energy for self-diffusion
R = Boltzmann constant
T = absolute temperature
σ = maximum stress
σ_0 = constant with dimensions of stress.

When $\sigma >> \sigma_0$ this equation becomes

$$\dot{\epsilon} = (\dot{\epsilon}_0/2) \exp [(\sigma/\sigma_0) - (E/RT)] \qquad (10)$$

or

$$\ln \dot{\epsilon} = \ln (\dot{\epsilon}_0/2) + (\sigma/\sigma_0) - (E/RT). \qquad (11)$$

For constant temperature, $d (\log \dot{\epsilon})/d\sigma = (2.303\ \sigma_0)^{-1}$.

Figure 19 is a plot relating stress to strain rate at three test temperatures. The slopes of these lines were used to give σ_0 values of 1.86 MN/m², 2.2 MN/m² and 5.56 MN/m² at -1.7°C, -5.6°C and -17.8°C respectively. At constant strain rate eq 11 gives $d\sigma/d(1/T) = E\sigma_0/R$. The two lines plotted in Figure 20 represent a strength-temperature dependence for each machine speed used for the compression tests. The slopes of these lines can be used to find the activation energy. For the lower machine speed, with an average strain rate of 5.5×10^{-3} sec^{-1}, the activation energy is found to be 49.1 kcal/mol (2.05×10^5 J/mol), 41.5 kcal/mol (1.73×10^5 J/mol) and 16.4 kcal/mol (6.86×10^4 J/mol) at -1.7°C, -5.6°C and -17.8°C respectively.

The values found for the activation energy for frozen silt in this investigation are higher than those found for ice by Dillon and Andersland and lower than those found for marble by Heard. These results also show agreement with the conclusion of Dillon and Andersland (1967) that higher activation energies are found at higher stresses and warmer temperatures. The activation energy found for frozen silt indicates that thermal activation may be useful for explaining the relationship between maximum stress and temperature at a constant strain rate.

CONCLUSIONS AND RECOMMENDATIONS

Uniaxial tests conducted on frozen Fairbanks silt in this investigation indicate that the strength is very sensitive to temperature. The compressive strength increased about one order of magnitude as the temperature was lowered from 0°C to -56.7°C. A higher rate of increase in strength was observed with tests run at higher strain rates. The tensile strength increased about one-half an order of magnitude as the temperature was lowered from 0°C to -56.7°C. The increased strength at lower temperatures was primarily due to the concurrent decrease in the quantity of unfrozen water and the increased strength of the ice matrix.

A relatively low sensitivity of strength to strain rate was observed with the tensile tests. At comparable temperatures and loading rates, the compressive strength found in this study is considerably higher than that reported by other investigators. This is probably because a relatively stiff testing machine was used in this investigation.

The initial tangent modulus increased about one order of magnitude with decreasing temperatures in the temperature range used in this study. Good agreement was found between the modulus results and those found in other investigations with uniaxial tests.

A general increase in specific energy with lower temperatures was found for the compression tests. For the tension tests, the specific energy decreased with lower temperatures. These results agree with those found in other studies. The activation energy for the slow compression tests was found to be 41.5 kcal/mol (1.74×10^5 J/mol). At comparable temperatures this is greater than the energy reported for ice in other investigations.

The results of this investigation provide information for the development of excavation techniques necessary for military operations in arctic regions. Additional testing of frozen silts at lower temperatures is needed to identify a plateau or peak in the compressive and tensile strengths. It is also recommended that uniaxial testing be done with other frozen soils and various types of ice to determine the effect of temperature upon their strength.

LITERATURE CITED

Butkovitch, T.R. (1954) Hardness of single ice crystals. U.S. Snow Ice and Permafrost Research Establishment (USA SIPRE) Research Paper 9. AD 041580.

Dillon, H.B. and O.B. Andersland (1967) Deformation rates of polycrystalline ice. In *Physics of snow and ice* (H. Oura, Ed.), *Proceedings, International Conference on Low Temperature Science*, 1966, Institute of Low Temperature Science, Hokkaido University, Sapporo, vol. I, pt. I, p. 313-27.

Fairhurst, C. (1970) Investigation of brittle fracture in frozen soil. U.S. Army Cold Regions Research and Engineering Laboratory (USA CRREL), Final Report, Contract no. DAAG-23-67-C-0023.

Glen, J.W. (1958) The mechanical properties of ice, I: The plastic properties of ice. *Advances in Physics*, vol. 7, p. 254-265.

Griffith, A.A. (1924) The theory of rupture. *Proceedings of the First International Congress for Applied Mechanics*, Delft, p. 55-63.

Hawkes, I. and M. Mellor (1970) Uniaxial testing in rock mechanics laboratories. *Engineering Geology*, vol. 4, no. 3, p. 217-218.

Hawkes, I. and M. Mellor (1972) Deformation and fracture of ice under uniaxial stress. *Journal of Glaciology*, vol. 11, no. 61, p. 103-131.

Haynes, F.D., J.A. Karalius and J. Kalafut (1975) Strain rate effect on the strength of frozen silt. USA CRREL Research Report 350. AD 021981.

Haynes, F.D. (1976) Effect of temperature on the strength of ice. (Unpublished).

Heard, H.C. (1963) Effect of large changes in experimental deformation of Yule marble. *Journal of Geology*, vol. 71, no. 2, p. 163.

Kaplar, C.W. (1953) Investigation of the strength properties of frozen soils. USA SIPRE Draft Report, vol. 2.

Kaplar, C.W. (1963) Laboratory determination of the dynamic moduli of frozen soils and ice. *Proceedings, Permafrost International Conference, Lafayette, Indiana, Building Research Advisory Board*, November, p. 293-301.

Kumar, A. (1968) The effect of stress rate and temperature on the strength of basalt and granite. *Geophysics*, vol. 33, no. 3, p. 501-510.

Landauer, J.K. (1955) Stress-strain relations in snow under uniaxial compression. *Journal of Applied Physics*, vol. 26, no. 12, p. 1493-1497.

McClintock, F.A. and J.B. Walsh (1963) Friction on Griffith cracks in rock under pressure. *Proceedings of the Fourth U.S. Congress Applied Mechanics*, p. 1015-1021.

Mellor, M. (1971) Strength and deformability of rocks at low temperatures. USA CRREL Research Report 294. AD 726372.

Mellor, M. and J. Smith (1966) Strength studies of snow. USA CRREL Research Report 168. AD 631717.

Offensend, F.L. (1966) The tensile strength of frozen soils. USA CRREL Technical Note (unpublished).

Peng, S.S. (1975) A note on the fracture propagation and time-dependent behavior of rocks in uniaxial tension. *International Journal of Rock Mechanics, Mining Science and Geomechanics* (Abstract), vol. 12, no. 4, p. 125-127.

Sayles, F.H. (1966) Low temperature soil mechanics. USA CRREL Internal Report 255 (unpublished).

Sayles, F.H. (1973) Triaxial and creep tests on frozen Ottawa sand. *Proceedings, Second International Permafrost Conference, Yakutsk, USSR.* National Academy of Sciences, Washington, D.C., p. 384-391.

Sayles, F.H. and N.V. Epanchin (1966) Rate of strain compression tests on frozen Ottawa sand and ice. USACRREL Technical Note (unpublished).

Sayles, F.H. and D. Haines (1974) Creep of frozen silt and clay. USA CRREL Technical Report 252. AD 784088.

Tice, A.R., D.M. Anderson and A. Banin (1973) The prediction of unfrozen water contents in frozen soils from liquid limit determinations. *Symposium on Frost Action on Roads*, Report 1, Norwegian Road Research Laboratory, Oslo, Norway, October, p. 329-344.

Tice, A.R., D.M. Anderson and A. Banin (1976) The prediction of unfrozen water contents in frozen soils from liquid limit determinations. CRREL Report 76-8. AD A026632.

Vialov, S.S. (Editor) (1965) The strength and creep of frozen soils and calculations for ice-soil retaining structures. USA CRREL Translation 76.

Wolfe, L.H. and J.O. Thieme (1964) Physical and thermal properties of frozen soil and ice. *Journal of the Society of Petroleum Technology*, March, p. 67-72.

☆U.S. GOVERNMENT PRINTING OFFICE: 1977—A-0703/150